Biomed Microdevices (2012) 14:435–441
DOI 10.1007/s10544-011-9620-9

Enhanced anesthetic propofol biochips by modifying molecularly imprinted nanocavities of biosensors

Chien-Chong Hong · Chih-Chung Lin · Chian-Lang Hong · Po-Hsiang Chang

Published online: 5 January 2012

Abstract This paper presents enhanced performance of anesthetic propofol biosensors by modifying molecularly imprinted nanocavities of biosensors. In this work, the relationship between molecularly imprinted nanocavities and performance of molecularly imprinted polymer (MIP) films is investigated. The morphological control of imprinted nanocavities on molecularly imprinted biosensors is done by adjusting polymer composition and polymerization process. The newly developed MIP biosensors are characterized using our developed microfluidic biochips and optical microsystems. Experimental results show that the sizes of molecularly imprinted nanocavities were reduced to 10 to 14 nm from 10 to 25 nm. The roughness of the MIP film surface was reduced to 2.5 nm from 6.6 nm. Smaller imprinted nanocavities have better molecular separation performance. The specificity and linearity of the anesthetic biosensors could be enhanced by adjusting morphology of imprinted nanocavities. The linearity and the sensitivity of the microfluidic biochip with an improved on-chip MIP biosensor have been enhanced from 0.9341 to 49.5 mV/mm^2.ml/μg, respectively, to 0.9782 and 176.9 mV/mm^2.ml/μg. The anesthetic propofol biosensor presented in this study is applicable to numerous fluidic-based disposable biochips.

Keywords Microfluidic biochip · Molecular imprinted nanocavity · Biosensor · Anesthetic propofol

C.-C. Hong (✉) · P.-H. Chang
BioMEMS and Nanobiosystems Lab., Department of Power Mechanical Engineering, National Tsing Hua University,
101, Sec. 2, Kuang Fu Rd.,
Hsinchu, Taiwan
e-mail: cchong@mx.nthu.edu.tw

C.-C. Lin
Department of Anesthesiology, Chang Gung Memorial Hospital,
Linkou, Taiwan

C.-L. Hong
Department of Anesthesiology, Chang Gung Memorial Hospital,
Chiayi, Taiwan

C.-L. Hong
Chang Gung University of Science and Technology,
Chiayi, Taiwan

1 Introduction

Anesthesia administration may be divided into administration of general anesthesia and regional anesthesia. The main purpose of all anesthesia techniques is to attenuate the patient's pain to enable smooth surgical activity. In addition to preoperative assessment, ongoing anesthesia monitoring during surgery is also required to ensure the safety of the patient. This depends on the subtle control of depth of anesthesia. When anesthesia is overdosed, it often results in a dip in blood pressure and heartbeat rate, delayed postoperative recovery, and death. However, when anesthesia depth is not enough, homeostasis is difficult to maintain. Moreover, higher than desired blood pressure and heartbeat rate leads to increase bleeding; or the patient even regains awareness because of insufficient anesthesia depth, which is quite dangerous during the surgery. Accurately determining the depth of anesthesia has been an important goal toward achieving a breakthrough in anesthesiology. This not only involves knowing the physiological status of the patient under anesthesia, but also controlling the doses required to keep the patient in the safest intraoperative condition until the surgery is complete. Propofol (2,6-di-isopropylphenol) is an intravenous anesthetic widely used in induction of anesthesia, total intravenous anesthesia, and sedation of

intensive care patients. Nowadays, pharmacokinetic programs are applied in target control infusion (TCI) for clinical anesthetic injection (Marsh et al. 1991; Schnider et al. 1999). To detect the concentration of propofol in the blood of a human body, high-performance liquid chromatography with UV detection (Teshima et al. 2001), high-performance liquid chromatography liquid chromatography with APCI-triple quadrupole mass spectrometry detection (Bajpai et al. 2004), and gas chromatography with mass spectrometry detection (Guitton et al. 1995) are conventionally used. However, not only are high-performance liquid chromatography and gas chromatography extremely expensive and difficult to access, but also the detection processes of both procedures are time-consuming and do not involve real-time detection. Therefore, neither conventional high-performance liquid chromatography nor gas chromatography is convenient for the doctor and patient to use. Clinically, more convenient access to monitoring propofol concentration in blood is required to avoid the adverse effects produced by excessive or insufficient propofol.

Traditional instruments are widely used in clinical laboratory for disease diagnostics. To gain insight and advance understanding on the biochemical substances of the human body, a vast array of biochemical assay techniques has been developed. In recent years, due to ever-increasing healthcare demands, conventional techniques can no longer satisfy certain needs. The problem mainly involves traditional analytical equipment requiring cumbersome sample pretreatment, and being bulky in size, complex in design, and expensive in cost. Moreover, such equipment is complicated, intended to be operated by professionals only, and unable to detect real time changes. There are growing demands on point-of-care testing for clinical diagnostics. The point-of-care assays can greatly improve the quality of medical care in the future. In order to further realize point-of-care test platforms for clinical diagnostics, developing microfluidic biochips with on-chip biosensors in response to these difficulties is urgent and imperative.

Biological molecules are always applied in the molecular recognition in biosensors. However, most of biological molecules have the difficulties in short shelf life, poor chemical resistant, thermal instability, high cost, and storage issue. Biosensors based on biological molecular recognition techniques are not suitable for point-of-care clinical diagnostics. Molecular imprinting is a newly developed technique that provides molecular assemblies of desired chemical structures and properties. Based on the concept of "tailor-made," a particular lock is designed to be unlocked by a specific key, mimicking the lock and key model of antigen-antibodies. Molecularly imprinted recognition structures can be artificially synthesized as needed. The advantages of such structures have stronger physical and chemical stabilities, long lifecycles, low cost. In the presence of a template molecule, functional monomers are polymerized and immobilized complementarily to this molecule. After polymerization, the template is removed by solvents. During these processes, a number of functional monomers are assembled in an orderly fashion with their functional groups placed at the desired sites within the cavities of the desired size. Therefore, molecular imprinted polymers with binding sites, with specific shape and functional group recognition, will enjoy high selectivity and high sensitivity sensing the target molecular compound. MIP technology has the advantages of high selectivity, high sensitivity, low-cost, and robustness (Haupt and Mosbach 2000). Molecularly imprinted polymers (MIPs) have been applied to many areas of chemistry, biochemistry, and medicine for sensing or separation of several analytes, such as chemicals, viruses, peptides, proteins, and cells (Bossi et al. 2001; Marty and Mauzac 2005; Ye and Mosbach 2008; He et al. 2007). The imprint effect and the influence of imprinting conditions on affinity, capacity, and heterogeneity in MIPs have been studied in the past (Rampey et al. 2004). Traditionally, MIPs have been prepared as bulk polymer monoliths and mechanically ground to obtain particles (Haupt 2003). The binding sites of MIPs are frequently damaged during the mechanical grounding process, though this usually resulted in damage to recognition sites and pores of uneven size. MIPs are preferred in thin films form than particles form in application of biosensors. Moreover, surface morphology of MIP films have been studied at the micro scale by several groups (Spivak et al. 2004; Richter et al. 2006; González et al. 2006; BelBruno et al. 2007; Campbell et al. 2009; Vendamme et al. 2009). However, specificity in morphology on imprinted nanocavities on a molecular scale has not been discussed in previous studies. In molecular imprinting, the target molecule acts as the template around which interacting and cross-linking monomers are arranged and co-polymerized to form imprinted nanocavities after polymerization and template removal. The morphology and functional groups of binding sites are strongly related to the selectivity of rebinding the target molecule.

In our previous work, we developed a prototype for a disposable microfluidic biochip with on-chip molecularly imprinted biosensors to enable the optical detection of the anesthetic propofol (Hong et al. 2010). In this paper, we examine the polymerization process and the morphology specificity of imprinted nanocavities on a molecular scale. We discuss enhancing microfluidic biochips with on-chip biosensors by adjusting the imprinted pore size, improving the specificity and linearity of the biosensors. The newly-developed biosensors are characterized using the microfluidic microsystem we developed to investigate surface morphology and anesthetic biosensor performance. Additionally, the developed biosensors are compared to a conventional spectrophotometer.

2 Materials and methods

Molecularly imprinted polymer (MIP) biosensors are widely used in many applications, such as separations or extractions, artificial antibodies, catalysts, and biosensors. Currently, an MIP film of the MIP biosensor is primarily manufactured by preparing a reaction solution including an imprinting molecule (which has functional groups and a size similar or identical to those of a target molecule), a functional monomer, a crosslinking agent, and an initiator. The MIP biosensor preparation entails: coating the reaction solution onto a substrate; curing and polymerizing the reaction solution to form a polymer film on the substrate; and extracting the imprinting molecule from the polymer film to form the MIP film having a plurality of recognition sites for binding to the target molecules. Once the molecular recognition layer is established in a biosensor, the recognized biochemicals signals must be subsequently transduced into treatable physical signals. The mechanism of optical sensing is based on the Beer-Lambert law. The method is used to determine concentration by linear correlation between light absorption and medium thickness and analyte concentration.

The work designed a set of biochip integrating optical microfluidics and MIP biosensors were, based on the microfluidic microchip platform being developed through BioMEMS and Polymer MEMS technologies. The microfluidic channel we designed, coupled to a syringe pump, may transport analyte and color reagent respectively into the active site of the MIP thin film. The analyte is captured by the MIP thin film, to be released and mixed by the color reagent. After primary purification, film recapturing, and further color reagent release, the system's specificity to analytes is enhanced. Finally, the mixture is examined using a laser diode and photodetector. The microfluidic biochip includes a disposable microfluidic biochip and MIP biosensors. As shown in Fig. 1(a) and (b), it is found with a schematic illustration of microfluidic biochips with on-chip molecularly imprinted biosensors for anesthetic sensing, and the microfluidic biochip was designed to precisely transport samples to the biosensor microchambers. The microfluidic biochip is a two-layer structure. The fluidic inlets and outlets are on the top layer. The microfluidic channel and the MIP biosensors are on the bottom layer. When propofol separation from the sample solution by the MIP biosensors is done, a color reagent was injected into the biosensor microchambers to react with propofol molecules. First, template molecules are imprinted on the MIP thin films. Then, the specific cavities are formed by releasing template molecules with solvent. The designed nanocavities have the ability to catch analyte molecules from sample in the microfluidic chamber. The mechanism of a microfluidic biochip is shown in Fig. 1(a). The microfluidic biochip is shown in Fig. 1(a–1). Above the microchannel is the reference biosensing site, and below it is the detecting biosensing site. Figure 1(a–2) is a diagram of sample injection. The reaction inside the detection site is shown in Fig. 1(b). The target molecule is absorbed by the MIP film, while non-target molecules cannot be adsorbed. Figure (1a–3) corresponds to the washed sample, the inside of the detection site is as Fig. (1b–2) only remains target molecules adsorbed by the MIP film. Figure (1a–4) is a diagram of color reagent injection, the inside of the detection site as shown as Fig. (1b–3) target molecules adsorbed by the MIP film are released, occurring color reaction with the reagent, and finally, as in Fig. 1(c) the sensing by optical mechanism of the chip reader. The sensing light emitted from the light source passes through the anesthetic molecules captured by the imprinted nanocavities on the molecularly imprinted biosensor, the molecularly imprinted biosensor, and the plastic chip substrate. The sensing light is then received by the photodetector. After that, the photodetector generates a detecting result based on the received sensing light.

For molecularly imprinting in this work, methacrylic acid and 4-vinylbenzeneboronic acid, they are used as functional monomers, while Ethylene glycol dimethacrylate and divinylbenzene are used as crosslinking agents. 2,6-dicholorimideqinone hydrochloride (Gibbs reagent), ethyleneglycoldimethacrylate EGDMA), methacrylic acid (MAA), and 1,1′-azo-bis(cyclohexanecarbonitrile) (ABCHC) were purchased from Sigma-Aldrich. MAA was used as a monomer, EGDMA as a crosslinker, and ABCHC as an initiator for polymerization. Cyclic olefin copolymers (Topas® COC 6015, Tg: 150° C) were chosen as chip substrates due to its low water absorption, and good resistance to several chemical solvents. In addition, the optical transmittance of COC plastic chips is 90%. A method for forming a molecularly imprinted polymer biosensor is shown in Fig. 2. Then, the MIP reaction solution was disposed in a space between the COC substrates and the spacer interposed between them. The reaction solution, which includes a solvent, an imprinting molecule, a functional monomer, an initiator, and a crosslinking agent, was irradiated through a photomask under UV exposure with an irradiation energy (wavelength: 365 nm, exposure power: 20 mW/cm^2), so the reaction solution undergoes polymerization to form patterned polymer films between the substrates. After the polymer films are formed on the lower substrate, extracting the imprinted template molecules from the surface of the polymer films by dipping in a methanol solution for 24 h so that a patterned molecularly imprinted polymer film is formed.

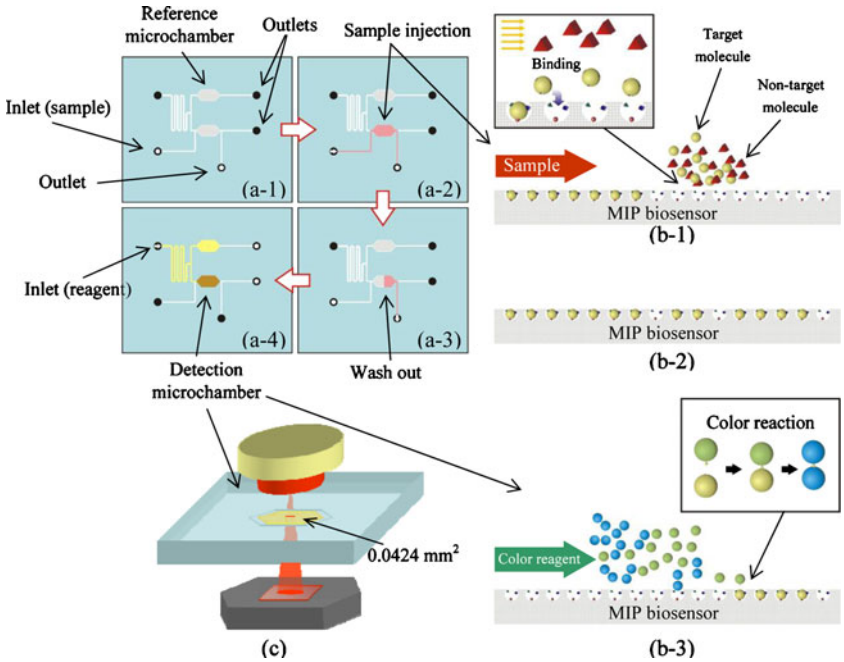

Fig. 1 Schematic illustration of the microfluidic biochip with on-chip MIP biosensors: (**a**) microfluidic procedure, (**b**) working principle, and (**c**) microfluidic sensing setup

In our previous work, the required UV energy for the polymerization of 25 μm-thick MIP film was 17 J/cm^2. After the polymerization of MIP using UV and the extraction of template molecules from MIP by a methanol solvent, the sizes of the imprinted nanocavities were between 13 and 47 nm [19]. The voids on the MIP film surface are significantly larger than the propofol molecule. Propofol molecules most likely combined and were imprinted in the cavity. This paper compares two types of MIP films and non-imprinted polymer (NIP) films, which are polymerized under different exposure energies. Type I MIP and NIP films are polymerized under exposure energy of 40 J/cm^2, while Type II MIP and NIP films are polymerized under exposure energy of 60 J/cm^2.

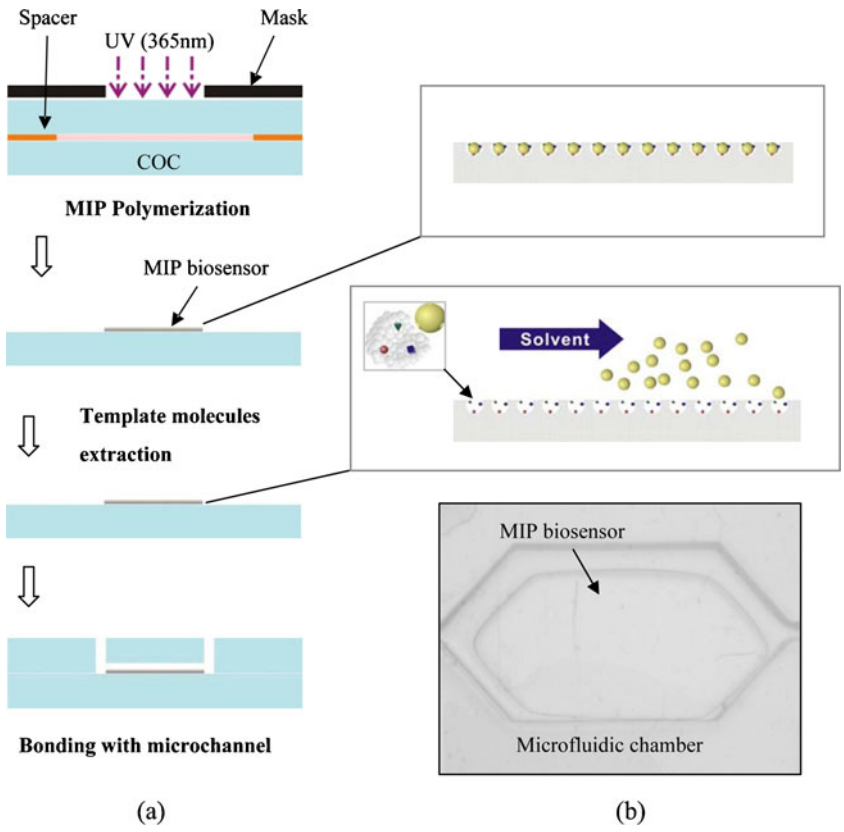

Fig. 2 Fabrication process: (**a**) fabrication and integration of MIP films with microfluidic biochips and (**b**) fabricated microfluidic biochips with on-chip MIP biosensors

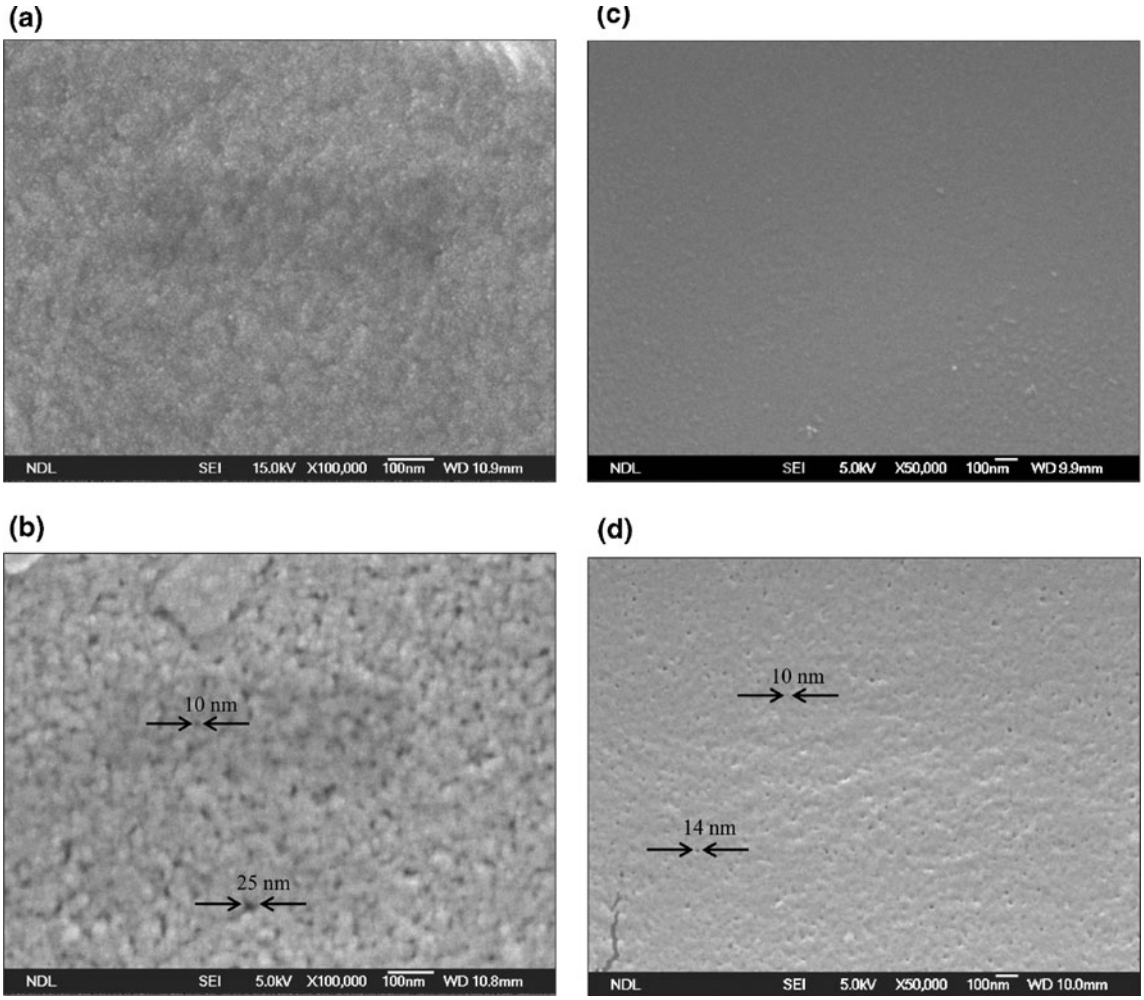

Fig. 3 SEM pictures of MIP and NIP films for two different polymerization conditions: (**a**) Type I NIP, (**b**) Type I MIP, (**c**) Type II NIP, and (**d**) Type II MIP

3 Experimental results and discussion

3.1 Surface morphology of MIP films and NIP films

The surface morphology of Type I and Type II MIP films were examined using a scanning electron microscope (SEM), as shown in Fig. 3. Both types of MIP films have greater surface porosity compared to NIP films. The nanocavities of MIP films are specific recognition sites formed by the template molecules. These imprinted nanocavities are larger than the individual molecules; therefore, the molecules must aggregate inside the recognition nanocavities. The sizes of the imprinted nanocavities can be determined from the SEM images. For Type I MIP films, the nanocavities are between 10 and 25 nm; for Type II MIP films the nanocavities are between 10 and 14 nm. The numbers of cavities per area for Type I MIP and Type II MIP are 390/mm^2 and 210/mm^2, respectively. Compared to those of Type II MIP films, Type I nanocavities are less homogeneous in size but higher in quantity. Comparisons between Type I and Type II MIP and NIP film surfaces indicate that both Type 1 film surfaces are coarser. In addition, these films were examined using an atomic force microscope (AFM). The roughness of the MIP film surface is reduced to 2.5 nm (Type II) from 6.6 nm (Type I), as tabulated in Table 1. Due to the greater surface roughness of Type I, the non-specific adsorption area is larger than that of Type II films.

Table 1 Surface morphology of type I and type II imprinted polymer films

	Average surface roughness R_a (nm)		Sizes of nanocavities (nm)		No. of cavities/area (#/mm^2)	
	MIP	NIP	MIP	NIP	MIP	NIP
Type I	6.6	2.9	10~25	0	390	0
Type II	2.5	1.0	10~14	0	210	0

Therefore, as the concentration increases in Type II MIP films, non-specific adsorption occurs more frequently with decreases in the specific adsorption.

3.2 Performance of microfluidic anesthetic biochips with MIP biosensors

The experimental setup for anesthetic concentration measurement using the designed biochip reader is shown in Fig. 4. The optical microsystem for propofol sensing was composed of 655 nm laser diodes, photodetectors, and a control circuit. In the experiments, the system was connected to a power supply and a PC-based DAQ system with a LabVIEW program for real-time continuous data recording.

The microsystem characterizes the dynamic response of propofol molecules released by color reagent reaction; the signal was detected by laser diodes and photodetectors. Furthermore, different concentrations of propofol samples were prepared mixing 98% propofol with methanol solvent. Using Gibbs's as a color reagent, 655 nm laser diodes were used to measure light absorption. The voltage of the photodetector was measured by the DAQ system, and increased immediately when the liquid sample filled the detection chamber. The syringe pump was then turned off to keep the propofol sample in the detection chamber for 60 s so that the separation of propofol molecules was conducted by MIP films and the liquid sample was removed with air injected into the microchamber. The voltage of the photodetector was decreased to the original value when the sample was completely removed. Afterwards, the color reagent was injected into the detection chamber and reference chamber (empty without MIP film) by a syringe pump. The pump was then turned off when the color reagent had filled both of the microchambers, and when the propofol molecules, captured by the MIP film earlier, began to release and react with the color reagent. Both light detection devices that were

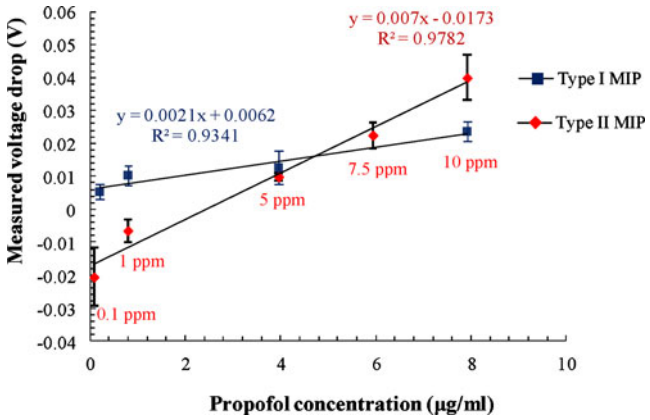

Fig. 5 Measurement results of our developed microfluidic biochips with Type I MIP biosensors and Type II MIP biosensors. (error bars of the measurements $n=3$)

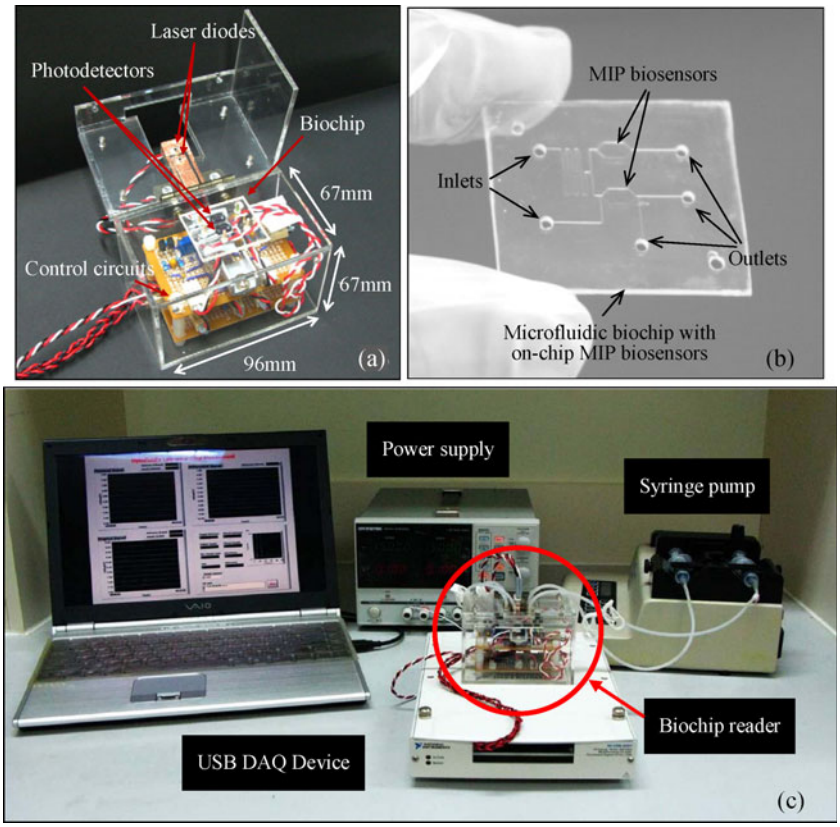

Fig. 4 Photographs of the microsystem and experimental setup: (**a**) biochip reader, (**b**) microfluidic biochip, and (**c**) experimental setup for anesthetic propofol concentration measurements

monitoring the reaction within the detection chamber and reference chamber were concurrently recorded by the DAQ system. The concentration of the sample using the microfluidic system was determined at the 60th second.

According to the measurements by the biochip reader, as shown in Fig. 5, the linearity and sensitivity of Type I MIP films are 0.9341 and 49.5 mV/mm^2.ml/μg, respectively. the linearity and sensitivity of Type II MIP films are 0.9782 and 176.9 mV/mm^2.ml/μg, respectively. The biochip with Type II MIP film exhibited excellent performance in linearity and sensitivity. Therefore, the proposed MIP film can be used in the MIP biosensor for detecting anesthetics, especially small molecule anesthetics, such as propofol. Furthermore, the MIP biosensor can exhibit relatively favorable sensitivity.

4 Conclusions

This study investigated the performance and surface morphology of the molecularly imprinted biosensor films. Surface morphology, which significantly affects the performance of the biosensor, can be improved by degree of exposure. Experimental results show that the sizes of molecularly imprinted nanocavities were reduced to 10 to 14 nm (Type II MIP) from 10 to 25 nm (Type I MIP). The roughness of the MIP film surface was reduced to 2.5 nm (Type II MIP) from 6.6 nm (Type I MIP). The microfluidic biochip for the application of anesthetic propofol detection has been characterized with the new developed Type II MIP biosensor. Smaller imprinted nanocavities have better molecular separation performance. The linear range was from 0.0792 to 7.918 μg/ml, with the lowest detected concentration being 0.0792 μg/ml. The linearity and the sensitivity of the microfluidic biochip with an improved on-chip MIP biosensor have been enhanced from 0.9341 to 49.5 mV/mm^2.ml/μg, respectively, to 0.9782 and 176.9 mV/mm^2.ml/μg. The performance of the anesthetic biosensors could be enhanced by adjusting morphology of imprinted nanocavities. The anesthetic propofol biosensor presented in this study is applicable to numerous fluidic-based disposable biochips.

Acknowledgements This research was supported by Chang Gung Memorial Hospital – National Tsing Hua University Joint Research (CMRPG380131 and CMRPG390131) and the National Science Council of Taiwan (NSC 98-2221-E-007-114).

References

L. Bajpai, M. Varshney, C.N. Seubert, D.M. Dennis, J. Chromatogr. B **810**, 291–296 (2004)
J.J. BelBruno, A. Richter, S.E. Campbell, U.J. Gibson, Polymer **48**, 1679–1687 (2007)
A. Bossi, S.A. Piletsky, E.V. Piletska, P.G. Righetti, A.P.F. Turner, Anal. Chem. **73**, 5281–5286 (2001)
S.E. Campbell, M. Collins, L. Xie, J.J. BelBruno, Surf. Interface Anal. **41**, 347–356 (2009)
G.P. González, P.F. Hernando, J.S.D. Alegría, Anal. Chim. Acta **557**, 179–183 (2006)
J. Guitton, M. Desage, A. Lepape, C.S. Degoute, M. Manchon, J.L. Brazier, J. Chromatogr. B: Biomed. Sci. Appl. **669**, 358–365 (1995)
K. Haupt, Anal. Chem. **75**, 376–383 (2003)
K. Haupt, K. Mosbach, Chem. Rev. **100**, 2495–2504 (2000)
C. He, Y. Long, J. Pan, K. Li, F. Liu, J. Biochem. Biophys. Methods **70**, 133–150 (2007)
C.-C. Hong, P.-H. Chang, C.-C. Lin, C.-L. Hong, Biosens. Bioelectron. **25**, 2058–2064 (2010)
B. Marsh, M. White, N. Morton, G.N.C. Kenny, Br. J. Anaesth. **67**, 41–48 (1991)
J.D. Marty, M. Mauzac, Adv. Polym. Sci. **172**, 1–35 (2005)
A.M. Rampey, R.J. Umpleby, G.T. Rushton, J.C. Iseman, R.N. Shah, K.D. Shimizu, Anal. Chem. **76**, 1123–1133 (2004)
A. Richter, U.J. Gibson, M. Nowicki, J.J. BelBruno, J. Appl. Polym. Sci. **101**, 2919–2926 (2006)
T.W. Schnider, C.F. Minto, S.L. Shafer, P.L. Gambus, C. Ansresen, D. B. Goodale, E.J. Youngs, Anesthesiology **90**, 1502–1506 (1999)
D.A. Spivak, R. Simon, J. Campbell, Anal. Chim. Acta **504**, 23–30 (2004)
D. Teshima, H. Nagahama, K. Makino, Y. Kataoka, R. Oishi, J. Clin. Pharm. Ther. **26**, 381–385 (2001)
R. Vendamme, W. Eevers, M. Kaneto, Y. Minamizaki, Polym. J. **41**, 1055–1066 (2009)
L. Ye, K. Mosbach, Chem. Mater. **20**, 859–868 (2008)